Effects of geometry on linear and non-linear gyrokinetic simulations, and development of a global version of the GENE code

X. Lapillonne[1], S. Brunner, T. Dannert, S. Jolliet, A. Marinoni, L. Villard, T. Görler, F. Jenko, and F. Merz

[1] Ecole Polytechnique Fédérale de Lausanne (EPFL), Centre de Recherches en Physique des Plasmas, Association Euratom-Confédération Suisse, CH-1015 Lausanne, Switzerland

xavier.lapillonne@epfl.ch

1. Gyrokinetic equation in general axisymmetric geometry

Working in field aligned coordinates (x: radial coordinate; y: binormal coordinate; z: parallel coordinate), the GENE [1, 2] code solves the gyrokinetic equation for the particle distribution function $f(x, y, z, v_\parallel, \mu) = f_0 + f_1$:

$$
\begin{aligned}
-\frac{\partial f_1}{\partial t} = & \left[\frac{1}{L_n} + \frac{1}{L_T}(v_\parallel^2 + \mu B - 3/2)\right] f_0 \frac{\partial \bar{\Phi}_1}{\partial y} && \} \text{ gradient driving term} \\
+ & \left[\frac{\partial \bar{\Phi}_1}{\partial x}\frac{\partial f_1}{\partial y} - \frac{\partial \bar{\Phi}_1}{\partial y}\frac{\partial f_1}{\partial x}\right] && \} \text{ nonlinear } \mathbf{E}\times\mathbf{B} \text{ drift} \\
+ & \frac{1}{B}\frac{\mu B + 2v_\parallel^2}{\sigma}\left(K_x \mathcal{G}_x + K_y \mathcal{G}_y\right) + \frac{v_\parallel^2 \beta}{\sigma B}\frac{dp}{dx}\mathcal{G}_y && \} \text{ curvature and pressure term} \\
+ & \alpha \frac{v_\parallel}{JB}\mathcal{G}_z - \frac{\mu\alpha}{2JB}\frac{\partial f_1}{\partial v_\parallel}\frac{\partial B}{\partial z} && \} \text{ trapping effects}
\end{aligned}
\tag{1}
$$

where $1/L_{Ti} = -d\ln T_i/dx$ and $1/L_n = -d\ln n/dx$, $\mathcal{G}_j = \partial_j f_1 + (\sigma_i/v_\parallel)\,\partial_j \bar{\Phi}_1\, \partial f_0/\partial v_\parallel$ for $j = (x, y, z)$, $\alpha_i = v_{Ti}/c_s$, $\sigma_i = Z_i T_e/T_i$, $\bar{\Phi}_1$ is the gyroaveraged electrostatic potential, and

$$
\begin{aligned}
K_x &= -\frac{g^{xx}g^{yz} - g^{yx}g^{xz}}{B^2}\frac{\partial B}{\partial z}, \\
K_y &= \frac{\partial B}{\partial x} - \frac{g^{xy}g^{yz} - g^{yy}g^{xz}}{B^2}\frac{\partial B}{\partial z},
\end{aligned}
$$

where the $g^{i,j} = \nabla u^i \cdot \nabla u^j$ are the metric coefficients and $J = [(\nabla x \times \nabla y)\cdot \nabla z]^{-1}$ is the Jacobian . The self-consistent electrostatic field is solved using the gyrokinetic Poisson equation :

$$
Z^2 \tau \left[1 - \Gamma_0(b)\right]\Phi_1 = \pi Z B \int J_0(\lambda) f_1 dv_\parallel d\mu - (\Phi_1 - \langle \Phi_1 \rangle)
$$

with $b = 1/(\tau B^2)\nabla_\perp^2$, $\lambda^2 = 2\mu/B\nabla_\perp^2$, $\nabla_\perp^2 = g^{xx}\partial^2/\partial x^2 + g^{yy}\partial^2/\partial y^2 + g^{xy}\partial^2/\partial x\partial y$ and $\langle\rangle$ the flux-surface averaging.

Note : Simulations are done with one kinetic ion species and adiabatic electrons. Equilibrium quantities are provided via the MHD equilibrium code CHEASE [3]. The equilibrium is set by analytically defining the shape of the last closed flux surface (LCFS), the current and the pressure profiles.

2. Cyclone case [4] benchmark, limitation of the $s-\alpha$ model [5]

Physical parameters at $\rho = \sqrt{\Phi/\Phi_{\text{edge}}} = 0.5$ (Φ is the toroidal flux): $q = 1.42$, $\hat{s} = (\rho/q)dq/d\rho = 0.8$, $\varepsilon = \rho a/R = 0.18$ (a : minor radius, R: major radius), $R\langle\nabla \ln T\rangle = 6.96$ and $R\langle\nabla \ln n\rangle = 2.23$.

- The $s-\alpha$ model approximates the straight field line angle to the poloidal angle $\Rightarrow$ growth rates differ by almost a factor 2 compared to results obtained using the MHD equilibrium.
- Ad-hoc concentric circular analytic equilibrium, which correctly treats the straight field line angle $\Rightarrow$ agreement within 10% with MHD equilibrium results.
- Good agreement with global code GYGLES [6], in the limit $\rho^* \to 0$.

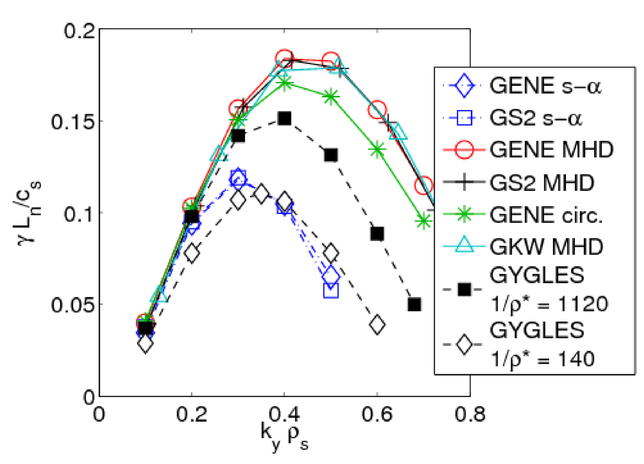

Figure 1: *Growth rate comparison for the Cyclone test case*

$\Longrightarrow$ True agreement is finally obtained between flux tube simulations with correct treatment of the geometry and global results in the appropriate $\rho^* \to 0$ limit.

3. Elongation and triangularity scan

- Same value of q and $\hat{s} = \rho/q dq/d\rho$ at $\rho = 0.5$; κ and δ are specified for the LCFS; $|\nabla \ln N| = 0$.

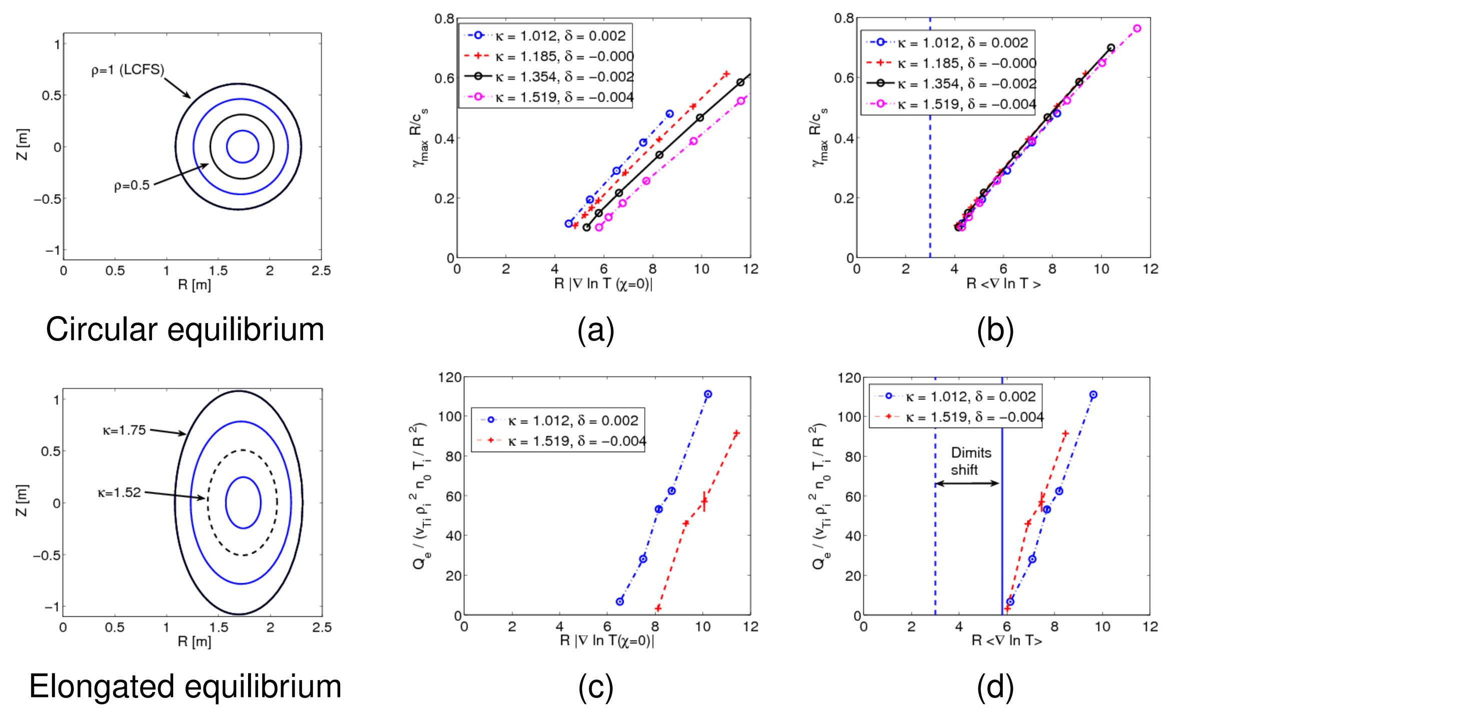

Figure 2: *Elongation scan at constant triangularity : (a,b) linear growthrate, (c,d) nonlinear electrostatic heat flux as a function of (a,c) the temperature gradient at $\chi = 0$ and (b,d) the flux surface-averaged temperature gradient $< \nabla \ln T >$. Note : κ and δ given at $\rho = 0.5$.*

$\Longrightarrow$ The dominant effect of elongation results from the modification of the spatial gradient, Fig. 2. (a) and (b). For simulations with similar linear growth rates there remains a small difference in the nonlinear heat flux, Fig. 2. (d).

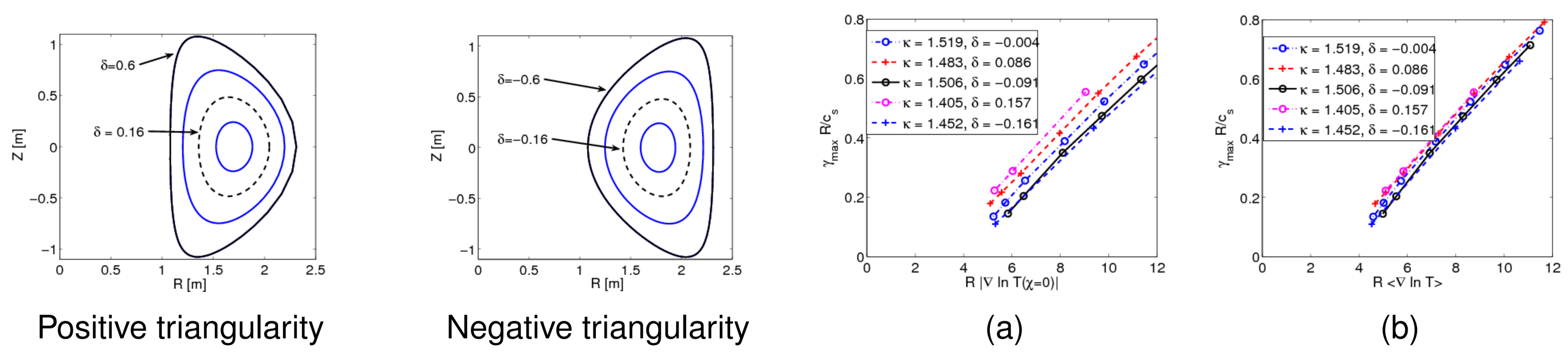

Figure 3: *Triangularity scan at constant elongation: Same as Fig. 2 (a) and (b)*

$\Longrightarrow$ The modification of the spatial gradient partly explains the effect of triangularity on linear growth rates, Fig. 3 (a) and (b). The remaining differences might arise from the modification of ∇B, see Fig. 4 (a) and (b).

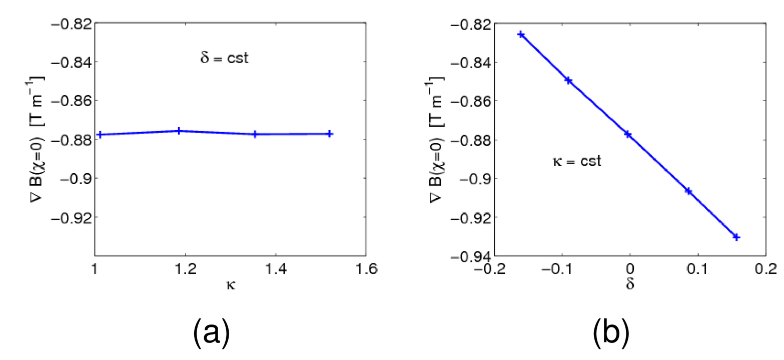

Figure 4: $\nabla B(\chi = 0)$ *for (a) different elongations and (b) different triangularities.*

4. Development of a global version of the GENE code

In order to address the issue of non-local effects in turbulent transport, a global version of the GENE code is under development. As a first step toward this goal, the x variation of equilibrium quantities will be introduced in the flux tube gyrokinetic equation (1) and in the field equations.

New features

The original Fourier representation for the radial direction has been replaced by a real space treatment, this has required to adapt :

- The radial derivatives: 4th order centered finite differences (same as for z derivatives).
- The gyro-averaging and the field solver : the Fourier space gyroaveraging $\bar{\Phi}(k_x, k_y, z, \mu) = J_0(k_x, k_y, z, \mu)\Phi(k_x, k_y, z)$ is replaced in the x direction by the real space gyroaveraging integral, for which a cubic-Hermite interpolation has been applied $\rightarrow$ banded Matrix operator on ϕ. A similar treatment is used for the field solver.
- Anti-aliasing: in the Fourier version of the code, when dealing with the nonlinear term, an anti-aliasing procedure is used to avoid pollution of the spectra by unresolved modes (may even lead to numerical instabilities). A scheme has been introduced to achieve similar anti-aliasing in real space.

The real space anti-aliasing

When working in Fourier space, the anti-aliasing procedure consists of two steps:

1) Extend the spectrum, and pad with zeroes before the nonlinear multiplication.

2) Remove the extended part of the spectrum from the nonlinear product.

These two steps correspond in real space to 1) an interpolation, followed by 2) a smoothing operation. When working in real space these two operations should remain local for practical reasons.

Effect of interpolation on spectrum

Let f be a periodic function represented on the initial N point grid and $\tilde{f}$ the corresponding interpolated function on the extended $2N$ point grid. In Fourier space one obtains:

$$
\hat{\tilde{f}}_k = H(k)\hat{f}_k, \qquad k = [-N, N].
$$

Noting that $\hat{f}_k$ is periodic with period N, $\hat{f}_k = \hat{f}_{k+N}$, a given mode $\hat{f}_k$ will therefore give rise to two modes in the $\tilde{f}$ spectrum :

$$
\hat{f}_k \rightarrow \begin{cases} 1)\hat{\tilde{f}}_k & = H(k)\hat{f}_k, \\ 2)\hat{\tilde{f}}_k + N & = H(k+N)\hat{f}_k, \end{cases}
$$

where the spectral extension function H is defined by the interpolation scheme and verifies $H(k) + H(k+N) = 1$.

Figure 5: *Spectral extension function H for Lagrange interpolation of various order n, Cubic Spline, Cubic Hermite compared to the box shaped function used in the Fourier version of the code.*

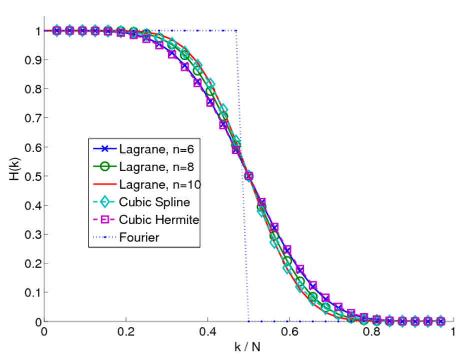

As the function $H(k)$ approaches the ideal box shape function, it has also been used to design the local real space smoothing operator.

Results for Cyclone parameters

Note : The following results are obtained with a version of the code which still uses Fourier treatment of the derivative and field solver but with the real space anti-aliasing procedure. A hyperdiffusion term, of the form $h_x(k_x\Delta_x)^4 f$, nonetheless needed to be added to the gyrokinetic equation to ensure stability.

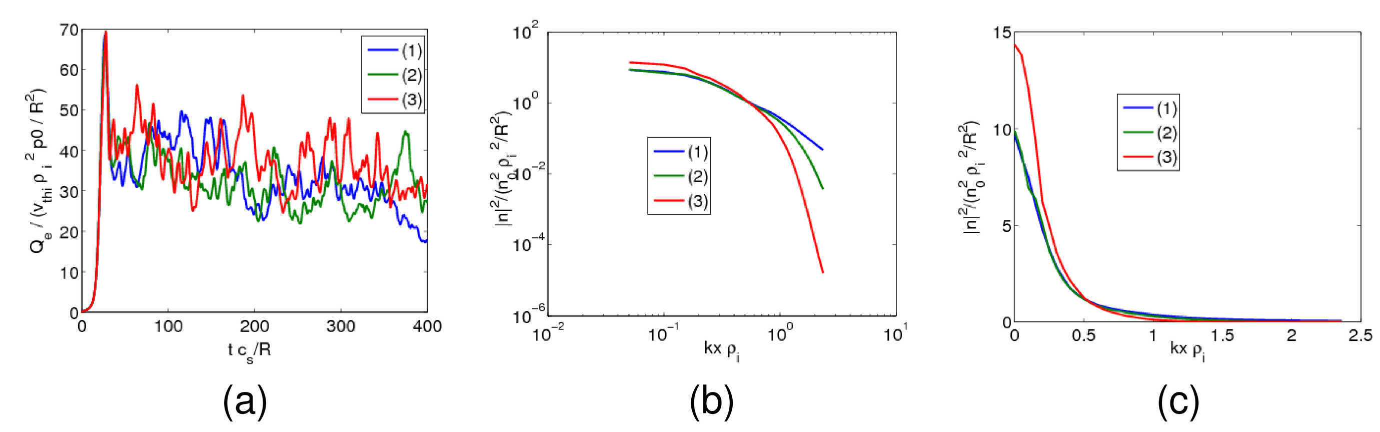

Figure 6: *(a) Electrostatic heat flux time trace,(b) k_x density spectrum in logarithmic and (c) linear scale. The different curves are obtained using (1) the standard Fourier anti-aliasing and $h_x = 0$, (2) the real space anti-aliasing with Lagrange interpolation of order 9 and $h_x = 0.6$, and (3) no anti-aliasing and $h_x = 4$.*

$\Longrightarrow$ The real space anti-aliasing enables to use a lower value of the hyperdiffusion coefficient h_x required to obtain a stable simulations compared to the case where no anti-aliasing was used. In addition the resulting k_x density spectrum is much closer to the simulations with Fourier space anti-aliasing.

References

[1] Jenko F., W. Dorland, M. Kotschenreuther, et al., *Phys. Plasmas*, **7**, 1904, 2000.

[2] Dannert T. and F. Jenko., *Phys. Plasmas*, **12**, 072309, 2005.

[3] H. Lütjens, A. Bondeson, and O. Sauter, Comp. Phys. Com. , **97**, 219, 1996.

[4] Dimits A., G. Bateman, M. Beer, et al., *Physics of Plasmas*, **7**, 969, 2000.

[5] Lapillonne X., Brunner S., Dannert T. et al., *"Limitations of the $s-\alpha$ equilibrium model for gyrokinetic computations of turbulence"* ,submited to Phys. Plamas.

[6] Fivaz M., Brunner S., de Ridder G. , et al., *Comp. Phys. Comm.*, **111**, 27, 1998.

Acknowledgement : This work was partly supported by the Swiss National Science Fondation.

Vienna, Austria, September 2008